Generation and detection of a spin entanglement in nonequilibrium quantum dots

Stefan Legel[1], Jürgen König[2], and Gerd Schön[1]
[1] *Institut für Theoretische Festkörperphysik and DFG-Center for Functional Nanostructures (CFN), Universität Karlsruhe, 76128 Karlsruhe, Germany and*
[2] *Institut für Theoretische Physik III, Ruhr-Universität Bochum, 44780 Bochum, Germany*

Spin entanglement between two spatially separated electrons can be generated in nonequilibrium interacting quantum dots, coherently coupled to a common lead. In this system entangled two-electron states develop which are Werner states with an imbalance between singlet and triplet probabilities. We propose a multi-terminal, multiply-connected setup for the generation and detection of this imbalance. In particular, we identify a regime in which the formation of spin entanglement leads to a cancellation of Aharonov-Bohm oscillations.

PACS numbers: 03.67.Mn,73.23.Hk,73.21.La,73.63.Kv

I. INTRODUCTION

The controlled generation and detection of entanglement of quantum states remains one of the fundamental challenges of quantum physics. Experiments with entangled photons have already entered the realm of advanced quantum communication and cryptography. In solid-state systems electron spins are considered as prime candidates for the demonstration of such effects. Spin degrees of freedom are only weakly coupled to the environment, which leads to long decoherence times [1, 2], and coherence lengths well exceeding the micrometer range. Several setups involving quantum dots have been proposed to create and detect pairs of spatially separated, spin-entangled electrons. The schemes rely, e.g., on the extraction of Cooper pairs from a superconductor [3], or the separation of a pair of entangled electrons from a singlet ground state of single [4, 5] or double quantum dots [6, 7]. Evidence of entanglement in these systems can be obtained from noise measurements [8] or coincidence detection [7]. In Ref. [9] a detection scheme was proposed where pure singlet and triplet states can be distinguished by Aharonov-Bohm interferometry.

In this article we analyze a setup with two spatially separated quantum dots, illustrated in Fig. 1, which allows the creation and detection of entanglement of spatially separated electron spins. The two dots are coupled coherently to a joint source electrode on the left and to two independent drain reservoirs at the top and bottom. When a bias voltage is applied, electrons are driven from the source via the dots to the drain electrodes. A nonequilibrium, mixed electronic state is created. For appropriate values of the voltage, due to the strong on-site Coulomb repulsion, a state with two electrons (one on each dot) has a high probability. It turns out to be of the form of a Werner state, with a strong enhancement of the singlet component, although singlet and triplet states are degenerate [10].

In order to detect the entanglement, an additional joint reservoir, closing the Aharonov-Bohm geometry, is coupled to the system. The current to this reservoir is studied in the cotunneling regime. Under certain conditions the entanglement leads to a suppression of the Aharonov-Bohm oscillations. Hence this part of the setup serves as probe of the state of the system and as detector for entanglement. Exploring the results in a wide parameter range we identify regimes where the double dot has a large probability to be in a singlet state. The predicted behavior provides a proof of concept for the entanglement generation in coherently coupled, nonequilibrium quantum dots.

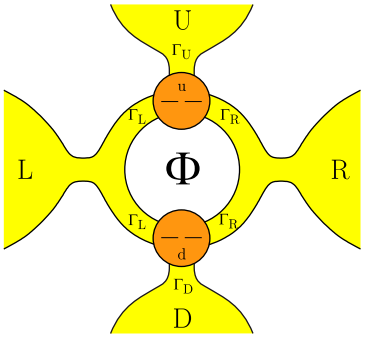

FIG. 1: Two quantum dots (u and d) coupled to a joint reservoir on the left hand side (L) and to two separate leads at the top and the bottom (U and D). The second joint reservoir on the right (R) closes the Aharonov-Bohm ring and is used to probe the state of the system.

II. MODEL

We consider the system shown in Figure 1. It consists of two single-level quantum dots, $i = \mathrm{u}, \mathrm{d}$, with strong on-site Coulomb repulsion U described by the Hamiltonian

$$H_{\mathrm{dots}} = \sum_{i\sigma} \varepsilon_i \, c^\dagger_{i\sigma} c_{i\sigma} + \sum_i U \, c^\dagger_{i\uparrow} c^\dagger_{i\downarrow} c_{i\downarrow} c_{i\uparrow} \, . \qquad (1)$$

The dots are coupled to joint reservoirs on the left and right forming an Aharonov-Bohm loop, and to two separate leads "up" and "down". The total system is then modelled by $H = H_{\mathrm{dots}} + H_{\mathrm{res}} + H_{\mathrm{t}}$ with the four leads,

$r = \mathrm{L}, \mathrm{R}, \mathrm{U}, \mathrm{D}$, with spin degenerate energies ε_{rk},

$$H_{\rm res} = \sum_{rk\sigma} \varepsilon_{rk}\, a^\dagger_{rk\sigma} a_{rk\sigma}\,, \tag{2}$$

and the four tunnel Hamiltonians $H_{\rm t} = H_{\rm tL} + H_{\rm tR} + H_{\rm tU} + H_{\rm tD}$. Tunneling between the upper dot and reservoir is simply described by

$$H_{\rm tU} = \sum_{k\sigma} \left[t_U\, c^\dagger_{u\sigma} a_{Uk\sigma} + {\rm h.c.} \right], \tag{3}$$

and similar for the lower pair. Tunneling between the joint leads on the left and the right, on the other hand, is sensitive to the phases of the matrix elements. Without loss of generality we can distribute them in a symmetric gauge,

$$\begin{aligned} H_{\rm tL} &= \sum_{k\sigma} \left[\left(t_{\rm Lu} {\rm e}^{-{\rm i}\varphi/4}\, c^\dagger_{{\rm u}\sigma} + t_{\rm Ld} {\rm e}^{+{\rm i}\varphi/4}\, c^\dagger_{{\rm d}\sigma} \right) a_{{\rm L}k\sigma} + {\rm h.c.} \right], \\ H_{\rm tR} &= \sum_{k\sigma} \left[\left(t_{\rm Ru} {\rm e}^{+{\rm i}\varphi/4}\, c^\dagger_{{\rm u}\sigma} + t_{\rm Rd} {\rm e}^{-{\rm i}\varphi/4}\, c^\dagger_{{\rm d}\sigma} \right) a_{{\rm R}k\sigma} + {\rm h.c.} \right]. \end{aligned} \tag{4}$$

All tunneling matrix elements are taken to be independent of spin and energy, and they can be chosen real and positive. The leads are assumed to be in local equilibrium, described by electrochemical potentials μ_r.

To keep the discussion transparent, we assume some symmetries. We set the upper and the lower reservoir to the same potential, $\mu_{\rm U/D} = \mu_{\rm U} = \mu_{\rm D}$, and restrict ourselves to degenerate dot levels, $\varepsilon = \varepsilon_{\rm u} = \varepsilon_{\rm d}$. We, furthermore, assume symmetric coupling strengths of the upper and lower dot to the left reservoir, $t_{\rm Lu} = t_{\rm Ld} = t_{\rm L}$, and similar for the right reservoir, $t_{\rm Ru} = t_{\rm Rd} = t_{\rm R}$, and we assume $t_{\rm U} = t_{\rm D} = t_{\rm U/D}$. Defining the tunneling strength by $\Gamma_r = 2\pi\, t_r^2\, N_r$, where N_r is the density of states of the relevant reservoir, we are left with three parameters $\Gamma_{\rm L}$, $\Gamma_{\rm R}$, and $\Gamma_{\rm U/D}$, which gives us enough freedom to tune the system into the interesting regimes. Double occupancy of each dot is suppressed by a strong Coulomb repulsion U, for simplicity assumed here to be larger than all other energy scales. However, the generalization to finite U is straightforward. We apply two bias voltages measured relative to $\mu_{\rm L} = 0$: a strong bias voltage between the left and the upper and lower reservoirs, $eV_{\rm U/D} = \mu_{\rm U/D}$, and a small transport voltage between the left and right reservoir, $eV_{\rm R} = \mu_{\rm R}$, used to probe the state of the system.

In essence, the preparation and measurement scheme analyzed in the following is based on two observations. First, the components of the density matrix which describe the doubly occupied system with one electron on each dot is a so-called Werner state, a mixture of a singlet and three equivalent triplet states. The distribution between singlet and triplet probabilities can be tuned in a certain range by the coupling strengths and the potentials applied to the system. For illustration we consider the state obtained immediately after charging the double dot with two electrons with opposite spin from the left reservoir

$$\begin{aligned} &(e^{-{\rm i}\varphi/4}\, c^\dagger_{{\rm u}\sigma} + e^{+{\rm i}\varphi/4}\, c^\dagger_{{\rm d}\sigma})(e^{-{\rm i}\varphi/4}\, c^\dagger_{{\rm u}\bar\sigma} + e^{+{\rm i}\varphi/4}\, c^\dagger_{{\rm d}\bar\sigma})|0\rangle \\ &\quad = e^{-{\rm i}\varphi/2}|\sigma\bar\sigma, 0\rangle + e^{+{\rm i}\varphi/2}|0, \sigma\bar\sigma\rangle + |\sigma, \bar\sigma\rangle - |\bar\sigma, \sigma\rangle\,. \end{aligned}$$

The minus sign in the last term is a direct consequence of the Fermi statistics. In view of this sign and the Pauli principle it is obvious that the equivalent expression for a pair of electrons with equal spin vanishes. A strong onsite Coulomb interaction prohibits double occupancy of each dot. Hence the state reduces to a perfectly entangled, pure singlet state

$$|{\rm S}\rangle = \left(|\sigma, \bar\sigma\rangle - |\bar\sigma, \sigma\rangle \right) / \sqrt{2}\,.$$

In equilibrium, however, the state has relaxed to a completely unentangled mixed state with uniformly distributed probabilities for singlet and triplets.

The second observation is that for the cotunneling rates the phases of the transport contributions for singlet and triplet states are shifted relative to each other by π. Hence they yield different interference patterns in the Aharonov-Bohm interferometer.

The strategy, therefore, is to use the subsystem composed of the left, upper, and lower reservoirs, and the dots to prepare the state of the system. In particular, we tune the ratio of singlet and triplet probabilities via the bias voltage $V_{\rm U/D}$. The signatures of this state in the transport are monitored by the Aharonov-Bohm interferometer, which is operated in the cotunneling regime for the tunneling to the right reservoir. The main message of this article is that for a setup with cascading coupling strengths, $\Gamma_{\rm L} \gg \Gamma_{\rm U/D} \gg \Gamma_{\rm R}$, an enhanced probability for singlet over triplet formation is associated with a suppression of the oscillations in the conductance of the Aharonov-Bohm probe.

III. PREPARATION OF STATIONARY ENTANGLED STATES

We investigate the system in the frame of the real-time diagrammatic technique Refs. [11, 12, 13] which allows us to go beyond an orthodox master equation approach. In particular we account for the quantum coherent time evolution of the double dot and focus on correlations between the electrons. The elements of the reduced density matrix are given by $p_\chi^{\chi'} = \langle \chi' | {\rm tr}_{\rm res}\, \rho | \chi \rangle$, where the reservoir degrees of freedom of the full density matrix are traced out, and χ and χ' label general many-body states of the double dot. For strong Coulomb repulsion, the reduced Hilbert space is spanned by nine basis states $|\chi_{\rm u}, \chi_{\rm d}\rangle$ with $\chi_i = 0, \uparrow, \downarrow$.

To describe the symmetries implied by tunneling we introduce a tailored basis. The state of the empty system and its probability are denoted by $|0, 0\rangle$ and p_0, respectively. A single electron of spin σ can occupy, with overall probability for single occupancy $p_1 = \sum_{i\sigma} p_{i\sigma}$, either the

upper or the lower dot, or, in general, any coherent superposition of these two. Thus, the corresponding block of the density matrix describes a quantum two-state system, which we express an isospin for each spin component, $\mathbf{I}_\sigma$. A natural basis are the two states with one electron in the upper or in the lower dot. However, in this basis the joint left and right reservoirs couple via the Hamiltonian (4) to the non-diagonal components $\mathbf{I}_\sigma \cdot \mathbf{m}_{\mathrm{L/R}}$ of the isospin, with

$$\mathbf{m}_{\mathrm{L/R}} = (\cos\frac{\varphi}{2}, \pm\sin\frac{\varphi}{2}, 0)\,, \tag{5}$$

which introduces a non-diagonal time evolution of the reduced density matrix. Electrons entering the double dot from the left reservoir generate an isospin polarization in direction of $\mathbf{m}_{\mathrm{L}}$, whereas electrons entering from the right are polarized in the direction of $\mathbf{m}_{\mathrm{R}}$. We further note, that due to the spin symmetry of the Hamiltonian the two spin components are completely equivalent. We will formulate equations for the expectation values of the isospin for either spin component, $\langle\mathbf{I}_\uparrow\rangle = \langle\mathbf{I}_\downarrow\rangle = \mathbf{I}_{\uparrow/\downarrow}$. To simplify expresssions we dropped in the last form the angular brackets.

The doubly occupied subspace with one electron on each dot is naturally spanned by the spin singlet $|\mathrm{S}\rangle$, which we find with probability p_{S}, and the three triplet states $|\mathrm{T}_+\rangle$, $|\mathrm{T}_0\rangle$, and $|\mathrm{T}_-\rangle$. Due to the spin symmetry of the Hamiltonian the three triplet states are equivalent and are occupied with equal probability $p_{\mathrm{T}_0} = p_{\mathrm{T}_\pm} = p_{\mathrm{T}}/3$. The corresponding block of the density matrix can be represented in the Werner form [14]

$$W(F) = F\,|\mathrm{S}\rangle\langle\mathrm{S}| + (1-F)\,\frac{\mathbb{1}_4 - |\mathrm{S}\rangle\langle\mathrm{S}|}{3}\,, \tag{6}$$

where the coefficient $F = p_{\mathrm{S}}/(p_{\mathrm{S}} + p_{\mathrm{T}})$ denotes the Werner fidelity. Values in the range of $1/2 < F \leq 1$ indicate a quantum correlated mixed state from which arbitrary entanglement can be distilled by suitable purification protocols [15, 16]. As we will show below, the Werner fidelity of the stationary state can be tuned in a certain range by the tunnel couplings and the applied bias voltage. Regimes with $F > 1/2$ are feasible if the double dot is predominantly charged from a common reservoir.

The kinetic equations for the reduced density matrix can be arranged in vector form with the diagonal probabilities collected in $\mathbf{p} = (p_0, p_1, p_{\mathrm{S}}, p_{\mathrm{T}})$ and the state of the singly occupied subspace specified by the isospin $\mathbf{I}_{\uparrow/\downarrow} = (I_x, I_y, I_z)$. In lowest order in the coupling strengths $\Gamma_{\mathrm{L}}, \Gamma_{\mathrm{R}}, \Gamma_{\mathrm{U/D}}$ we obtain

$$\begin{aligned}
\frac{\mathrm{d}}{\mathrm{d}t}\mathbf{p} &= \sum_{r=\mathrm{L,R,U/D}} \Gamma_r \begin{pmatrix} -4\,f_r & 1-f_r & 0 & 0 \\ 4\,f_r & -1-f_r & 2-2\,f_r & 2-2\,f_r \\ 0 & f_r/2 & -2+2\,f_r & 0 \\ 0 & 3\,f_r/2 & 0 & -2+2\,f_r \end{pmatrix} \mathbf{p} + \sum_{r=\mathrm{L,R}} \Gamma_r \begin{pmatrix} 4-4\,f_r \\ -4+8\,f_r \\ 2\,f_r \\ -6\,f_r \end{pmatrix} (\mathbf{I}_{\uparrow/\downarrow}\cdot\mathbf{m}_r) \\
\frac{\mathrm{d}}{\mathrm{d}t}\mathbf{I}_{\uparrow/\downarrow} &= \sum_{r=\mathrm{L,R}} \Gamma_r \left[f_r\,p_0 + \left(f_r - \frac{1}{2}\right)\frac{p_1}{2} + (1-f_r)\,\frac{p_{\mathrm{S}}}{2} - (1-f_r)\,\frac{p_{\mathrm{T}}}{2} \right] \mathbf{m}_r - \sum_{r=\mathrm{L,R,U/D}} \Gamma_r\,(1+f_r)\,\mathbf{I}_{\uparrow/\downarrow}\,,
\end{aligned} \tag{7}$$

where the Fermi distributions $f_r = 1/(e^{\beta(\varepsilon-\mu_r)}+1)$ in the respective reservoirs are evaluated at the dots' energy ε. The Equations (7) extend our earlier work [10], where we considered a double-dot system coupled to three reservoirs, but without the Aharonov-Bohm probe and right reservoir.

To generate and detect a singlet-triplet imbalance, the system parameters have to be chosen specifically. First, the tunnel coupling to the right lead should be much weaker than the other ones, $\Gamma_{\mathrm{R}} \ll \Gamma_{\mathrm{L}}, \Gamma_{\mathrm{U/D}}$, in order to ensure that the state of the double dot is not affected by the measurement via the interferometer. Furthermore, only a small bias voltage is applied across the Aharonov-Bohm ring, and the dot levels are kept off resonance such that the flux-sensitive linear conductance is dominated by cotunneling processes. Finally, in order to find with large probability two electrons in the system, the rate for charging should be much larger than for discharging, $\Gamma_{\mathrm{L}} \gg \Gamma_{\mathrm{U/D}}$.

In the following, we compare two situations:
(i) For vanishing bias voltage between the left and upper/lower reservoirs, the double dot remains in equilibrium, and $F = 1/4$. This defines the reference for comparison.
(ii) By applying a high bias voltage between the left and upper/lower reservoirs, we generate a singlet-triplet imbalance with $F > 1/2$.

IV. PROBING THE SINGLET-TRIPLET IMBALANCE

Cases (i) and (ii) lead to significantly different interference signatures in the transport through the Aharonov-Bohm ring. While the first one shows a strong flux dependence and large amplitude of the Aharonov-Bohm os-

cillations, they are suppressed in the second case, where the Werner fidelity approaches 1/2 if the double dot is predominantly occupied with two electrons. To demonstrate this difference we calculate the linear conductance through the Aharonov-Bohm interferometer. The contribution to first order in the coupling strength is evaluated within the diagrammatic technique. It turns out to be small due to our choice of parameters (compare also Figure 3). For the dominant second-order contribution we calculate the stationary density matrix according to (7) and obtain the cotunneling rates from Fermi's Golden rule [17, 18, 19]

$$(2\pi)^2 N_{\rm L} N_{\rm R} \sum_{\chi_{\rm f},k_{\rm f}} \left| \sum_n \frac{\langle \chi_{\rm f}\, k_{\rm f}|H_{\rm t}|n\rangle\langle n|H_{\rm t}|\chi_{\rm i}\, k_{\rm i}\rangle}{\omega - E_n} \right|^2 . \quad (8)$$

Here the initial double-dot state is denoted by $\chi_{\rm i}$, and all possible final states are summed over. The energy E_n of the intermediate virtual state $|n\rangle$ is either 0, ε or 2ε, and ω is the energy of the incoming lead electron.

Gathering all cotunneling terms corresponding to the four scenarios where the dot system is empty ($\chi = 0$), occupied with a single electron with isospin $\mathbf{I}_{\uparrow/\downarrow}$ ($\chi = 1$), or occupied with two electrons either in a singlet ($\chi = {\rm S}$) or a triplet ($\chi = {\rm T}$) state, we find the second order contribution to the linear conductance $G_{\rm R} = \partial I_{\rm LR}/\partial V_{\rm R}|_{V_{\rm R}=0}$,

$$G_{\rm R}^{(2)} = -\frac{e^2}{h}\, g(\varphi)\, {\rm Re} \int {\rm d}\omega\, \frac{\Gamma_{\rm L}\Gamma_{\rm R}}{(\omega - \varepsilon + i0^+)^2}\, f'(\omega) . \quad (9)$$

The Aharonov-Bohm flux dependence is included in the dimensionless conductance $g(\varphi) = \sum_\chi g_\chi(\varphi)$, with

$$g_0(\varphi) = 2\,(1+\cos\varphi)\, p_0(\varphi) \quad (10a)$$

$$g_1(\varphi) = 2\,(3-\cos\varphi)\, p_1(\varphi) + 16\,(\mathbf{m}_{\rm L} - \mathbf{m}_{\rm R})\cdot \mathbf{I}_{\uparrow/\downarrow} \quad (10b)$$

$$g_{\rm S}(\varphi) = \left(\frac{1}{2} - \frac{1}{4}\cos\varphi\right) p_{\rm S}(\varphi) \quad (10c)$$

$$g_{\rm T}(\varphi) = \left(\frac{1}{2} + \frac{1}{4}\cos\varphi\right) p_{\rm T}(\varphi) \quad (10d)$$

The flux sensitivity of the conductance is twofold. First, the phase factors from the tunneling Hamiltonian are taken into account in the coherent summation of processes in the cotunneling rates (8). In particular, as discussed in [9], the phase dependence of the contributions from an initial singlet and triplet state (Equations (10c) and (10d)) are shifted relative to each other by π. We emphasize that these results rely on the degeneracy of singlet and triplets. All four constitute equivalently possible final states of cotunneling processes with an initially doubly occupied system. If there was a large singlet-triplet energy splitting with transitions between singlet and triplet states being suppressed, then $g_{\rm S,T}(\varphi) = (1+\cos\varphi)\, p_{\rm S,T}/4$ without any distinction between the contributions.

The second kind of flux dependence results from the stationary state distribution of the system. In general nonequilibrium situations, the reduced density matrix, represented by p_0, p_1, $\mathbf{I}_{\uparrow/\downarrow}$, $p_{\rm S}$, and $p_{\rm T}$, is influenced by the Aharonov-Bohm probe and becomes phase sensitive. This effect is weak for weak tunnel coupling $\Gamma_{\rm R} \ll \Gamma_{\rm L}, \Gamma_{\rm U/D}$ where the state of the system is only weakly influenced by the AB-probe. In the limit $\Gamma_{\rm L} \gg \Gamma_{\rm U/D} \gg \Gamma_{\rm R}$ and the double dot charged from the left reservoir the isospin points approximately in direction of $\mathbf{m}_{\rm L}$ such that $g_1(\varphi) \approx 2\,(3-\cos\varphi)\, p_1 - 16\,(1-\cos\varphi)\,|\mathbf{I}_{\uparrow/\downarrow}|$.

We compare now the two scenarios (i) and (ii). For low dot energies in an equilibrium situation, $\varepsilon \ll \mu_r$, the double dot is mainly occupied with two electrons with $p_{\rm T} \approx 3/4$ and $p_{\rm S} \approx 1/4$. As a consequence, in this equilibrium reference situation there is a good visibility of the Aharonov-Bohm oscillations,

$$g^{\rm (i)}(\varphi) \approx \frac{1}{2} + \frac{1}{8}\cos\varphi\,. \quad (11)$$

In contrast, for strong bias voltage, the phase dependence is suppressed. To see this, we expand the density matrix for a strong asymmetry in the coupling to the left, and the upper and lower reservoirs, $x = \Gamma_{\rm U/D}/\Gamma_{\rm L} \ll 1$, and obtain $p_0 = \mathcal{O}(x^2)$, $p_1 = 4x/3 + \mathcal{O}(x^2)$, $\mathbf{I}_{\uparrow/\downarrow} \approx x/6\,\mathbf{m}_{\rm L} + \mathcal{O}(x^2)$, $p_{\rm S} = 1/2 - x/2 + \mathcal{O}(x^2)$, and $p_{\rm T} = 1/2 - 5x/6 + \mathcal{O}(x^2)$. Thus, the dimensionless conductance approaches

$$g^{\rm (ii)}(\varphi) \approx \frac{1}{2} + \frac{\Gamma_{\rm U/D}}{\Gamma_{\rm L}}\left(\frac{14}{3} - \frac{29}{12}\cos\varphi\right) . \quad (12)$$

For strong asymmetry, $\Gamma_{\rm U/D} \ll \Gamma_{\rm L}$, the oscillations of the singlet and triplet terms cancel each other and the phase dependence of the conductance vanishes. This suppression of the Aharonov-Bohm amplitude allows us to detect the singlet-triplet asymmetry generated in system.

We remark that if the system is prepared in a state with maximal entanglement, $p_{\rm S} = 1$ or $p_{\rm T} = 1$, as considered in Ref. [9], then the visibility of the Aharonov-Bohm oscillations would be even twice as large as in equilibrium, $g = \frac{1}{2} \mp \frac{1}{4}\cos\varphi$. For a steady-state scenario considered in this paper, however, it is not possible to have both a large overall probability of double occupancy of the double dot and a maximal singlet-triplet imbalance at the same time. To optimize the probability for double occupancy we choose $\Gamma_{\rm L} \gg \Gamma_{\rm U/D}$, for which $p_{\rm S} = p_{\rm T} = 1/2$, which indicates finite but not maximal entanglement.

The plots in Figure 2 display the linear conductance up to second order in the coupling strength based on a full solution of the stationary equations (7). If the system is close to equilibrium, $|eV_{\rm U/D}| \ll k_{\rm B}T$, the triplet probability is large ($F \approx 1/4$), and the conductance is dominated by a positive $\cos\varphi$ kind of oscillation (compare Equation (11)). In contrast, the interference is suppressed if the system is driven into a singlet-triplet imbalance by charging the double dot from the joint left lead, $F \approx 1/2$.

A finite singlet-triplet relaxation reduces the imbalance between singlet and triplet in the stationary state, and the Aharonov-Bohm oscillations are restored. To estimate the influence of spin flip and dephasing we in-

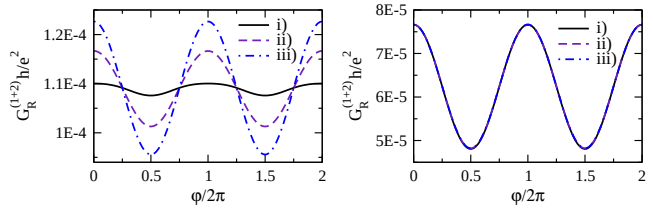

FIG. 2: The linear conductance of the Aharonov-Bohm subsystem up to second order in the coupling strength is plotted versus the Aharonov-Bohm phase. The parameters are $\Gamma_{\rm L} = 1\,k_{\rm B}T$, $\Gamma_{\rm U/D} = 0.1\,k_{\rm B}T$, $\Gamma_{\rm R} = 0.01\,k_{\rm B}T$, $\varepsilon = -10\,k_{\rm B}T$ and $|eV_{\rm R}| \ll k_{\rm B}T$. For strong bias voltage between the left and the upper/lower reservoirs, $eV_{\rm U/D} = -20\,k_{\rm B}T$ (left plot), and in equilibrium (right plot), the ideal system (i) is compared to results for singlet-triplet decay rates of (ii) $\Gamma_{\rm ST} = 0.5\,\Gamma_{\rm U/D}$ and (iii) $\Gamma_{\rm ST} = 10\,\Gamma_{\rm U/D}$.

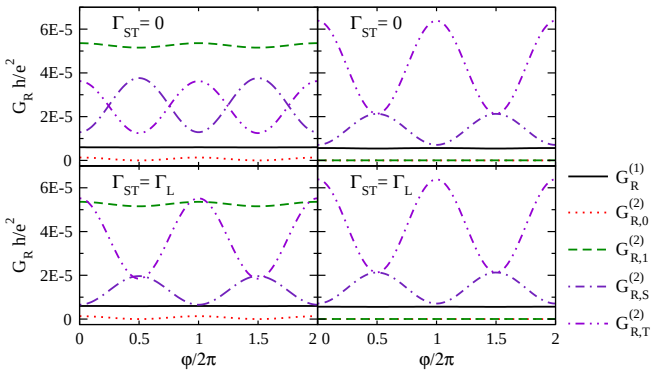

FIG. 3: The individual contributions to the linear conductance are plotted with and without singlet-triplet relaxation. The first order, $G_{\rm R}^{(1)}$, and second order terms, $G_{{\rm R},\chi}^{(2)}$, are specified for equilibrium (right plots) and for strong bias voltage, $eV_{\rm U/D} = -20\,k_{\rm B}T$ (left plots). The parameters are $\Gamma_{\rm L} = 1\,k_{\rm B}T$, $\Gamma_{\rm U/D} = 0.1\,k_{\rm B}T$, $\Gamma_{\rm R} = 0.01\,k_{\rm B}T$, $\varepsilon = -10\,k_{\rm B}T$ and $|eV_{\rm R}| \ll k_{\rm B}T$.

troduce phenomenological transition rates between singlet and triplets. For simplicity we choose all of them equal to $\Gamma_{\rm ST}$. To observe a significant suppression of the Aharonov-Bohm oscillations a relaxation rate smaller than the current rate between source and drain is required, i.e. $\Gamma_{\rm ST} < \Gamma_{\rm U/D}$ in our case.

In Figure 3 the first and second order conductance contributions are plotted individually. The transport supported by the equilibrium state is dominated by the second order triplet contribution and the Aharonov-Bohm oscillations are well visible. The singlet-triplet relaxation does not affect the behavior. If the electrons are strongly driven into the double dot from the joint left reservoir, a singlet-triplet imbalance forms and the oscillations of the singlet and triplet contributions cancel each other. A finite relaxation rate partially destroys the imbalance and the cancellation. The conductance supported by the singly occupied states becomes quite strong for a large bias voltage, however, its phase dependence is weak since for strongly asymmetric coupling the isospin is parallel to $\mathbf{m}_{\rm L}$ with $|\mathbf{I}_{\uparrow/\downarrow}| \approx 1/8\,p_1$ such that $g_1 \approx 4\,p_1$.

V. CONCLUSIONS

Here we proposed a setup for the generation and detection of spin entanglement between two spatially separated electrons. A bias voltage applied across a double-dot system with strong onsite Coulomb repulsion, coherently coupled to a joint source electrode and individually coupled to separate drains, creates an imbalance between singlet and triplet probabilities. An asymmetry in the coupling of source and drain increases the overall probability to find two excess electrons in the double dot system and for them to form a Werner state. The underlying mechanism of entanglement generation relies on the specific nonequilibrium situation and is fundamentally different from those schemes in which two electrons are extracted from a singlet ground state.

To detect the singlet-triplet imbalance we added an Aharonov-Bohm probe, obtained by coupling a second joint reservoir coherently to the double dot. The enclosed flux controls the interference pattern which depends on the state of the double dot. In particular, the cotunneling transport through the Aharonov-Bohm ring is sensitive to an imbalance in the singlet-triplet distribution.

We compared two situations: For vanishing bias voltage between the joint source and the drain reservoirs the double dot is in equilibrium, and singlet and triplet are uniformly distributed, and the Aharonov-Bohm conductance is strongly flux dependent. On the other hand, by applying a strong bias voltage a singlet-triplet imbalance is generated, and the Aharonov-Bohm oscillations are suppressed. By choosing asymmetric couplings we can ensure that the double dot was predominantly occupied with two electrons.

For an experimental realization one needs a geometry with spatial separation of the dots shorter than the phase coherence length. Finite decoherence due to spin-orbit effects, hyperfine coupling or coupling to some other bath will reduce the overall visibility of the Aharonov-Bohm oscillations. Nevertheless, the extra suppression of the Aharonov-Bohm oscillations for strong bias voltage as compared to equilibrium will indicate a singlet-triplet asymmetry. The probability to find the system occupied with two electrons can be enhanced by tuning the dot levels well below the Fermi energy of the probe and choosing a strong asymmetry in the coupling of source and drain. For the detection of a suppressed phase dependence caused by a singlet-triplet imbalance a tunneling rate between source and drain much larger than the spin decoherence time is required.

Acknowledgments

We acknowledge stimulating discussions with G. Burkard, P.W. Brouwer, J. Weis, J. Martinek, Y. Gefen, T. Löfwander, and E. Prada. This work was supported by the Landesstiftung Baden-Württemberg via the Kompetenznetz Funktionelle Nanostrukturen, and DFG via SFB 491 and SPP 1285.

[1] Koppens F H L, Folk J A, Elzerman J M, Hanson R, Willems van Beveren L H, Vink I T, Tranitz H P, Wegscheider W, Kouwenhoven L P, and Vandersypen L M K, 2005 Control and detection of singlet-triplet mixing in a random nuclear field *Science* **309** 1346.

[2] Petta J R, Johnson A C, Taylor J M, Laird E A, Yacoby A, Lukin M D, Marcus C M, Hanson M P, and Gossard A C 2005 Coherent manipulation of coupled electron spins in semiconductor quantum dots *Science* **309** 2180.

[3] Recher, Sukhorukov E V, and Loss D 2001 Andreev tunneling, Coulomb blockade, and resonant transport of nonlocal spin-entangled electrons *Phys. Rev.* B **63** 165314.

[4] Oliver W D, Yamaguchi F, and Yamamoto Y 2002 Electron entanglement via a quantum dot *Phys. Rev. Lett.* **88** 037901.

[5] Saraga D S and Loss D 2003 Spin-entangled currents created by a triple quantum dot *Phys. Rev. Lett.* **90** 166803.

[6] Hu X and Das Sarma S 2004 Double quantum dot turnstile as an electron spin entangler *Phys. Rev.* B **69** 115312.

[7] Blaauboer M and DiVincenzo D P 2005 Detecting entanglement using a double-quantum-dot turnstile *Phys. Rev. Lett.* **95** 160402.

[8] Burkard G, Loss D, and Sukhorukov E V 2000 Noise of entangled electrons: Bunching and antibunching *Phys. Rev.* B **61** R16303.

[9] Loss D and Sukhorukov E V 2000 Probing entanglement and nonlocality of electrons in a double-dot via transport and noise *Phys. Rev. Lett.* **84** 1035.

[10] Legel S, König J, Burkard G, and Schön G 2007 Generation of spin entanglement in nonequilibrium quantum dots *Phys. Rev.* B **76** 085335.

[11] König J, Schmid J, Schoeller H, and Schön G 1996 Resonant tunneling through ultrasmall quantum dots: Zero-bias anomalies, magnetic-field dependence, and boson-assisted transport *Phys. Rev.* B **54** 16820.

[12] König J and Gefen Y 2002 Aharonov-Bohm interferometry with interacting quantum dots: Spin configurations, asymmetric interference patterns, bias-voltage-induced Aharonov-Bohm oscillations, and symmetries of transport coefficients *Phys. Rev.* B **65** 045316.

[13] Pohjola T, Schoeller H, and Schön G 2001 Orbital and spin Kondo effects in a double quantum dot *Europhys. Lett.* **54** 241.

[14] Werner R F 1989 Quantum states with Einstein-Podolsky-Rosen correlations admitting a hidden-variable model *Phys. Rev.* A **40** 4277.

[15] Bennett C H, DiVincenzo D P, Smolin J A, and Wootters W K 1996 Mixed-state entanglement and quantum error correction *Phys. Rev.* A **54** 3824.

[16] Linden N, Massar S, and Popescu S 1998 Purifying noisy entanglement requires collective measurements *Phys. Rev. Lett.* **81** 3279.

[17] Averin D V and Nazarov Y V 1990 Virtual electron diffusion during quantum tunneling of the electric charge *Phys. Rev. Lett.* **65** 2446.

[18] Averin D V and Nazarov Y V 1992 *Single Charge Tunneling, NATO ASI Series 294* H Grabert and M H Devoret (Plenum Press).

[19] Akera H 1993 Aharonov-Bohm effect and electron correlation in quantum dots *Phys. Rev.* B **47** 6835.